JPPIPA 10(6) (2024)

Jurnal Penelitian Pendidikan IPA

Journal of Research in Science Education

http://jppipa.unram.ac.id/index.php/jppipa/index

Characterization of Fiber Bragg Grating Accelerometer for Underwater Vibration Detection

Juan Michael Kane Gani[1], Retno Wigajatri Purnamaningsih[1*], Sasono Rahardjo[2]

[1] Departemen Teknik Elektro, Universitas Indonesia, Depok, Indonesia.
[2] Pusat Riset Elektronika, Badan Riset dan Inovasi Nasional, Jakarta, Indonesia.

Received: April 23, 2024
Revised: June 15, 2024
Accepted: June 25, 2024
Published: June 30, 2024

Corresponding Author:
Retno Wigajatri Purnamaningsih
retno.wigajatri@ui.ac.id

DOI: 10.29303/jppipa.v10i6.7760

Abstract: In this paper, the results of the characterization of a Fiber Bragg Grating (FBG) Accelerometer for detecting vibrations underwater are reported. The FBG Accelerometer, consisting of three FBGs, is utilized to detect underwater vibrations in three-dimensional directions. A water pump, with positions varied from 0 to 10 cm, is employed as the vibration source. Furthermore, the experimental results are presented in the form of the peak wavelength shift reflected by the FBG ($\Delta\lambda_B$) and frequency. From the experiment results, it is shown that with increasing distance, $\Delta\lambda_B$ decreases linearly with successive gradients of 0.0058 nm/cm; 0.0059 nm/cm; and 0.0045 nm/cm. for FBG X, Y, and Z. It is also shown that with increasing distance, there is a decrease in frequency from 50 Hz for FBGs X, Y, and Z to 39 Hz; 38 Hz; and 40 Hz for FBGs X, Y, and Z respectively.

Keywords: Fiber Bragg Grating; Vibration Detection; Bragg Wavelength

Introduction

Vibration detection plays a crucial role in observing and analyzing seismic activities on the Earth's crust (Hou et al., 2023) and has various applications such as detecting vibrations on the ocean surface (Lan et al., 2022) and identifying potential tsunamis and earthquakes (Duggal et al., 2022).

In Indonesia, natural events such as earthquakes occur quite frequently on several islands, including Jawa, (Supendi et al., 2022), Sulawesi (Jena et al., 2020), Kalimantan, Maluku (Sianipar et al., 2022), and other smaller islands (Ramdani et al., 2019). This is due to Indonesia's location surrounded by three tectonic plates: the Eurasian Plate, the Indo-Australian Plate, and the Pacific Plate (Wibowo et al., 2023). Various methods have been developed to create sensor systems that detect underwater earthquakes and swiftly transmit information to land (Z. Li, 2021). One of the developments implemented is Indonesia Tsunami Early Warning System (Ina-TEWS) in the form of buoys. Buoy is a floating device on the sea surface that records changes in water level (Martínez-Osuna et al., 2021). Although this system is relatively new, it has its weaknesses, namely the high cost of procuring and maintaining buoys, and its inability to provide information regarding the scale of the impending tsunami (Made, 2018).

Therefore, due to these issues, FBG can become an alternative sensor to detect underwater earthquake vibrations. Currently, Badan Riset dan Inovasi Nasional (BRIN) is developing an FBG sensor system called the Indonesia Cable-Based Tsunameter (Ina-CBT), which can be integrated into the existing Ina-TEWS system. The FBGs are installed on the seabed with lengths reaching hundreds of kilometers and connected to a base station located on the coast. FBG has a very long operational lifespan because it does not rely on batteries and can transmit data in larger quantities and shorter timeframes. Research on the utilization of FBG in water has been conducted, which examines the effects of temperature on the Bragg wavelength shift (Kustianto et al., 2023).

As a continuation of that research, this study characterizes an FBG accelerometer for detecting

How to Cite:
Gani, J. M. K., Purnamaningsih, R. W., & Rahardjo, S. (2024). Characterization of Fiber Bragg Grating Accelerometer for Underwater Vibration Detection. *Jurnal Penelitian Pendidikan IPA*, *10*(6), 3221–3227. https://doi.org/10.29303/jppipa.v10i6.7760

underwater vibrations as a basis for developing underwater sensors. The FBG accelerometer consists of three FBGs that will detect vibrations in three-dimensional directions: X, Y, and Z. Subsequently, an analysis of the changes in Bragg wavelength and frequency for each FBG is conducted.

Method

The FBG sensor operates based on the principle of interference that occurs between the transmitted (Yan & Liang, 2020) and reflected light (L. Zhang et al., 2022) by the grating structure within the optical fiber (L. Wang et al., 2022).

This results in a specific wavelength being reflected by the FBG (H. Wang et al., 2021) while other wavelengths pass through the grating. When light passes through the grating structure, a specific wavelength, known as the Bragg wavelength, will be reflected back (Qian et al., 2021). Bragg wavelength (λ_B) can be determined as Formula 1:

$$\lambda_B = 2n_{eff}\,\Lambda \quad (1)$$

where n_{eff} is the effective core index of refraction (Le et al., 2022), and Λ is the spatial period of the grating (Shen et al., 2023). When the FBG is subjected to disturbances such as vibration, pressure, or temperature, the value of λ_B changes correspondingly (Nguyen et al., 2023). The change in Bragg wavelength ($\Delta\lambda_B$) can be described as Formula 2:

$$\frac{\Delta\lambda_B}{\lambda_B} = (1 - pe)\Delta\varepsilon + (af + \xi f)\,\Delta T \quad (2)$$

where $\Delta\varepsilon$ is the longitudinal strain variation (J. Li et al., 2022), ΔT is the temperature increment, pe is the elasto-optical coefficient of the fiber (Dong et al., 2023), af is the the coefficient of thermos-optic (H. Zhang et al., 2018), dan ξf is the coefficient of thermal expansion of the fiber (Pan et al., 2019). When the FBG experiences vibration, a change in strain occurs within the FBG. This change in strain affects λ_B, resulting in changes of $\Delta\lambda_B$ (T. Yang et al., 2021).

Figure 1 shows the FBG Accelerometer consisting of 3 FBGs: FBG X, FBG Y, and FBG Z. FBG X has λ_B of 1544 nm, FBG Y has λ_B of 1529 nm, and FBG Z has λ_B of 1540 nm. Figure 2 shows the experimental setup for vibration detection measurements. In this setup, the FBG is connected to the optical interrogator (3S-BS01). The function of the interrogator is to send light to the FBG and demodulate the optical signal reflected back from the FBG (Guo et al., 2023). After the demodulation process is completed, the information is displayed on a laptop (Y. Li et al., 2022).

A regulated DC power supply (PAN 35-20A) provides 5 V and 0.3A to the interrogator processing system for optical signal demodulation. For the vibration source, a 60 W water pump (PW-105) is used to generate vibrations underwater (J. Li et al., 2023). A container box with a capacity of 120 liters serves as a small pool where the FBG accelerometer is placed for underwater experiments.

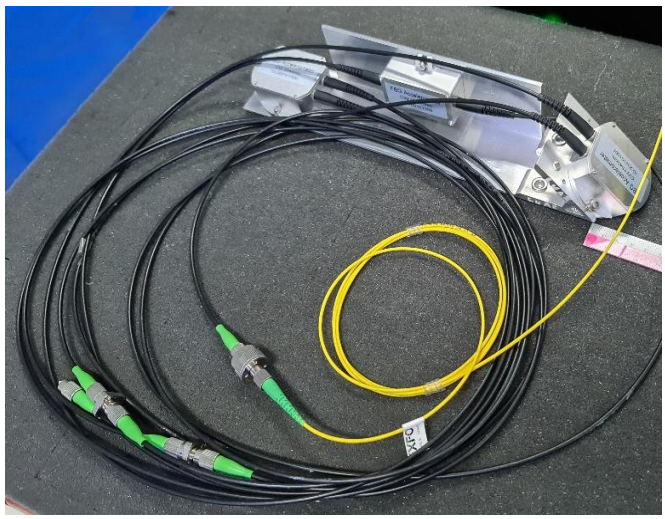

Figure 1. FBG Accelerometer

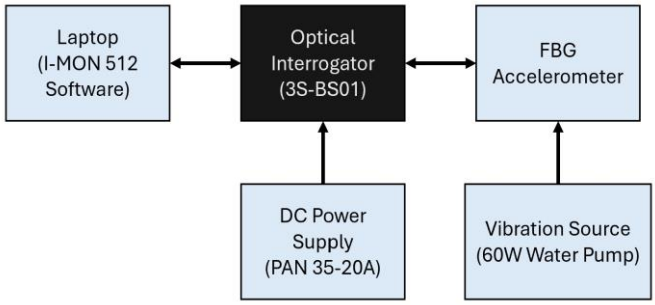

Figure 2. Schematic of experiment setup

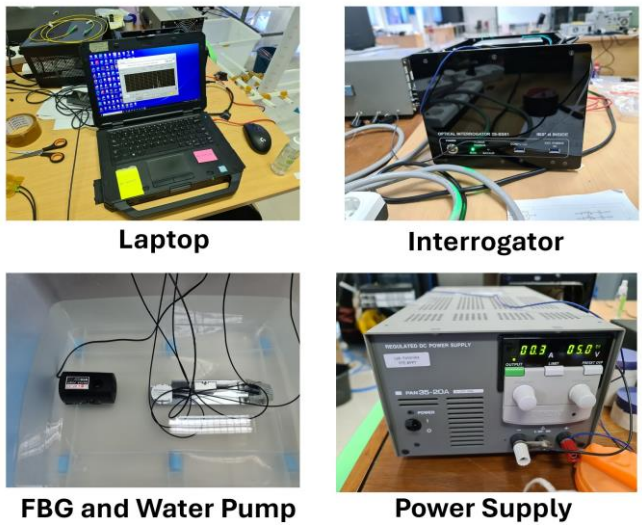

Figure 3. Supporting components of experiment

The water level in the container box reaches 17 cm. This height is sufficient to submerge both the FBG and the water motor. For each measurement, different distance values are used for each FBG, starting from 0, 2, 4, 6, 8, and 10 cm (Le et al., 2023). Figures 4 to 6 show an experimental setup measuring vibrations from the vibration source with FBG X, Y, and Z at the distance of 10 cm.

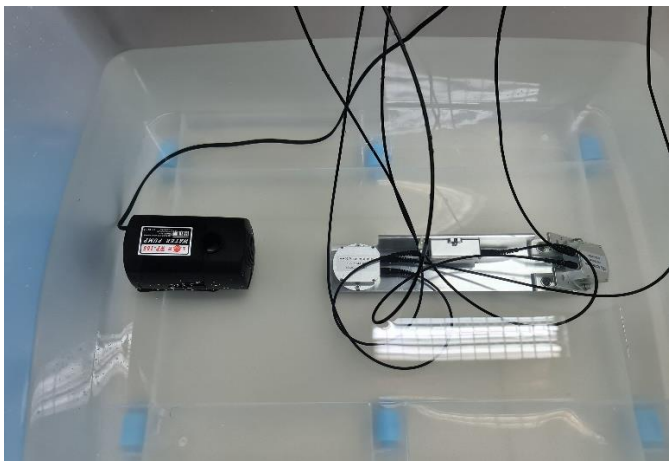

Figure 4. Vibration source at 10 cm from FBG X

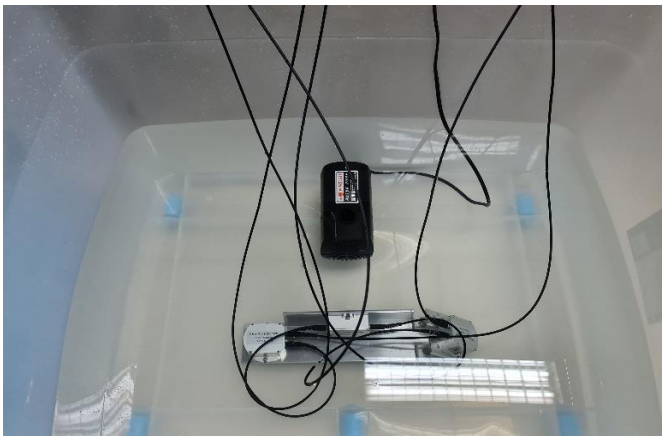

Figure 5. Vibration source at 10 cm from FBG Y

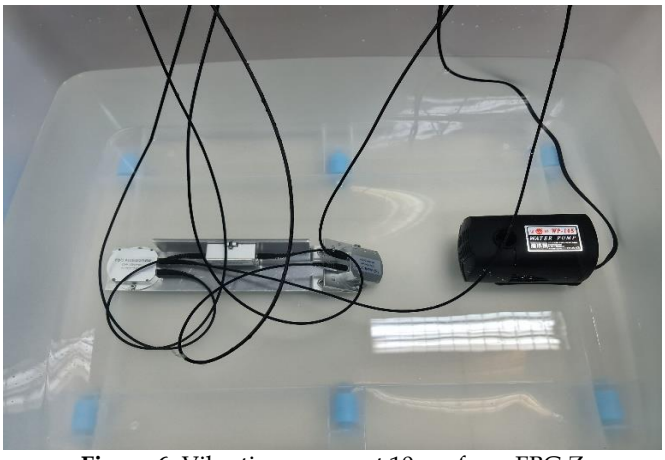

Figure 6. Vibration source at 10 cm from FBG Z

The software used to display the demodulation results is Ibsen Photonics I-MON 512 USB Evaluation Software. Figures 7 and 8 show two graphs: a spectrum graph and a wavelength graph. During the experiment, the spectrum graph needs to be kept constant at all times to ensure that the results of each measurement remain consistent and accurate (X. Yang et al., 2020). Wavelength graph shows λ_B of FBG X, Y, and Z.

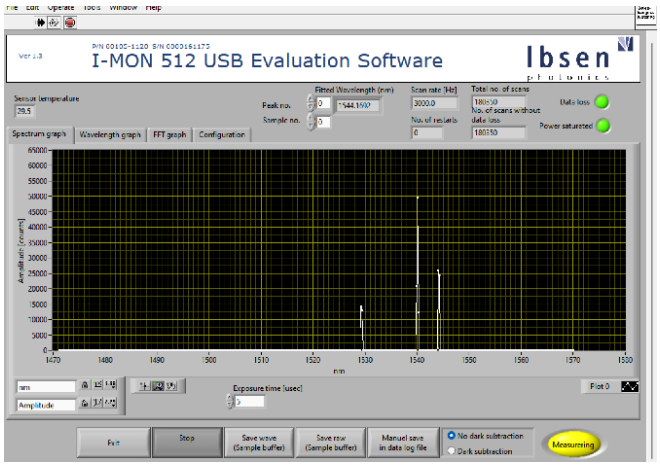

Figure 7. Spectrum Graph View

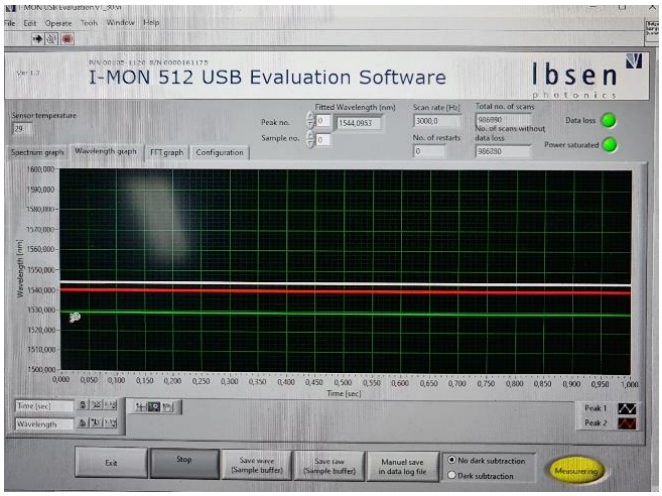

Figure 8. Wavelength Graph View

Result and Discussion

For each measurement, data was collected for 1 minute, obtaining 600 data points with a sampling time of 0.1 seconds for FBG X, Y, and Z. When FBG X is stationary and not subjected to any vibration disturbances, λ_B of FBG X is 1544.1399 nm, λ_B of FBG Y is 1529.1390 nm, and λ_B FBG Z is 1540.0208 nm.

When water pump is running, vibrations are generated and causing changes to λ_B of FBG X, Y, dan Z. Figure 9 shows the changes in λ_B values of FBG X, Y and Z at the distance of 0, 2, 4, 6, 8, and 10 cm. When the water pump is at 0 cm from FBG, λ_B of FBG X is 1544.2520

nm, λ_B of FBG Y is 1529.5455 nm, and λ_B of FBG Z is 1529.5455 nm. When water pump is 10 cm from FBG, all three values of λ_B decrease. The λ_B of FBG X is 1544.1878 nm, λ_B of FBG Y is 1529.4825 nm, and λ_B of FBG Z is 1540.0658 nm. The measurement results indicate that as the distance increases, the changes in λ_B for FBG X, Y, and Z decreases.

For frequency measurements, the FFT function of the I-MON software was used to gather frequency data received by each FBG from distances of 0, 2, 4, 6, 8, and 10 cm. Figure 10 shows the changes in distance against the frequency values received by FBG X, Y, and Z. At the distance of 0 cm, frequency received by FBG X, Y, and Z is 50 Hz. At the distance of 10 cm, frequency received by FBG X is 39 Hz, FBG Y is 38 Hz, and FBG Z is 40 Hz. The measurement results indicate that as the distance increases, the frequency values received by FBG X, Y, and Z decrease.

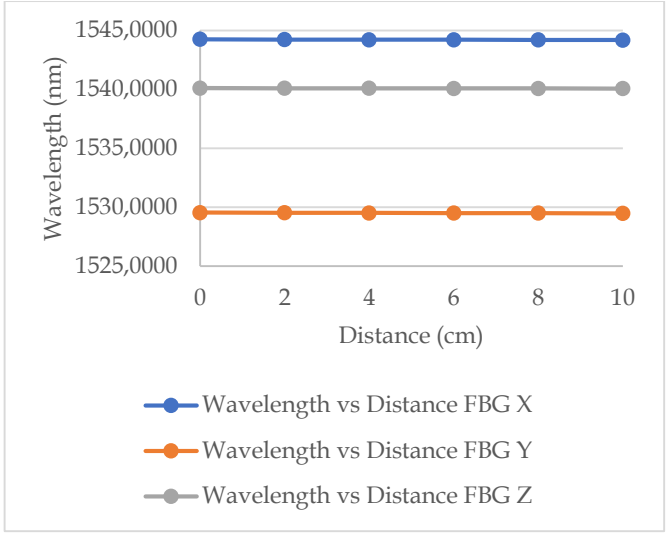

Figure 9. The change in λ_B of FBG X, Y, and Z due to distance change from 0 to 10 cm

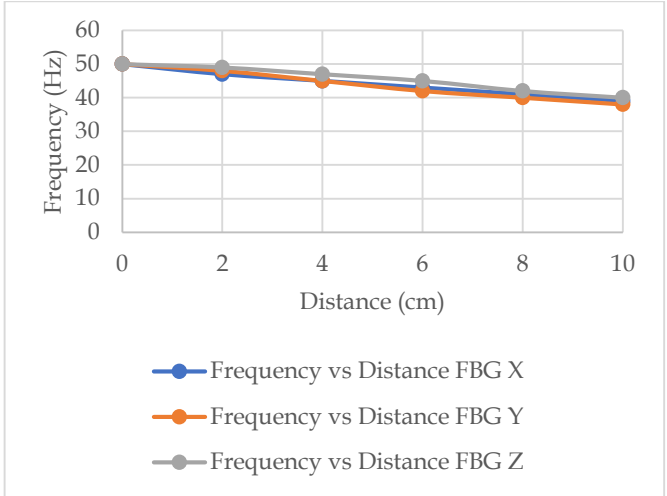

Figure 10. The change in frequency of FBG X, Y, and Z due to distance change from 0 to 10 cm

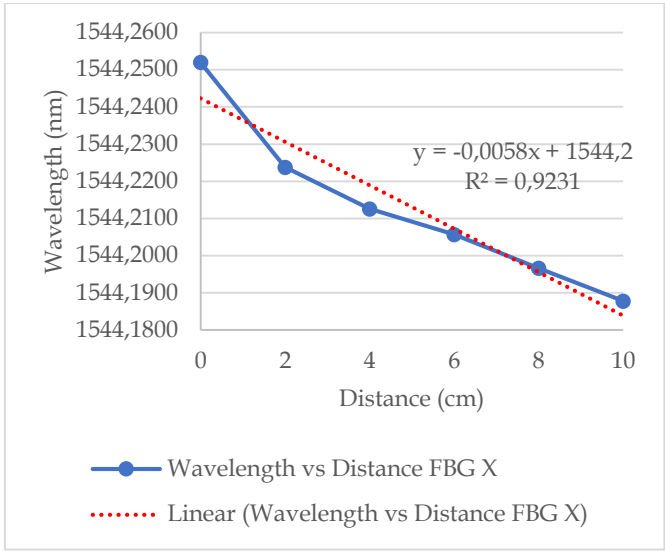

Figure 11. The change in $\Delta\lambda_B$ of FBG X due to distance change from 0 to 10 cm

A linear regressions analysis is conducted on the change in λ_B or $\Delta\lambda_B$ of FBG X, Y, and Z with respect to the distance. Figure 11 shows a graph of $\Delta\lambda_B$ for FBG X. From linear regression analysis, there's gradient of decline with a value of 0.0058 nm/cm and R-squared value of 92.31%. Figure 12 shows a graph of $\Delta\lambda_B$ for FBG Y. From linear regression analysis, there's gradient of decline with a value of 0.0059 nm/cm and R-squared value of 96.47%. Figure 13 shows a graph of $\Delta\lambda_B$ for FBG Z. From linear regression analysis, there's gradient of decline with a value of 0.0045 nm/cm and R-squared value of 98.82%.

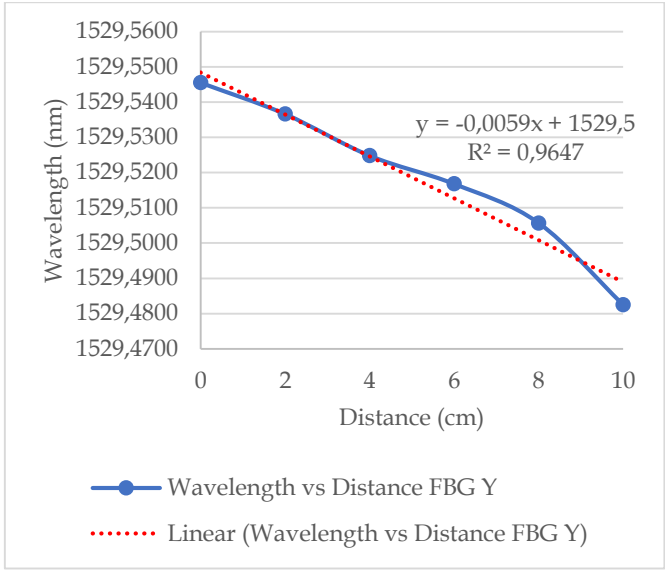

Figure 12. The change in $\Delta\lambda_B$ of FBG Y due to distance change from 0 to 10 cm

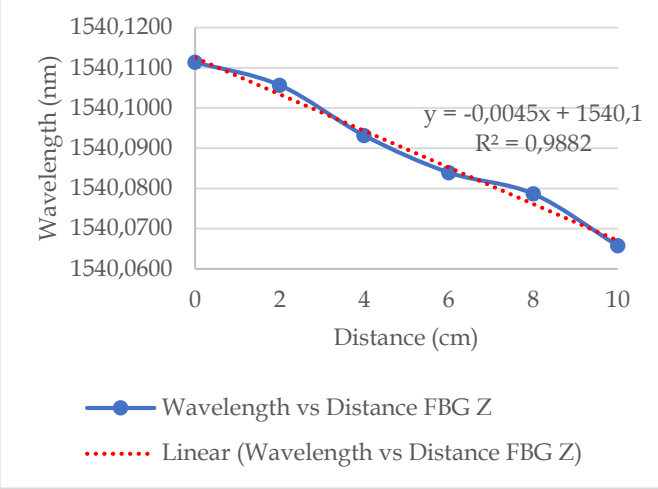

Figure 13. The change in $\Delta\lambda_B$ of FBG X due to distance change from 0 to 10 cm

FBG Accelerometer has been extensively explored in vibration measurement (Feng et al., 2015; Parida et al., 2019; X. Wang et al., 2018; Teng et al., 2024 Xu et al., 2024). These experiments used one or two FBGs and were conducted on air with shaking table to simulate vibrations produced by a source. The novelty of this specific experiment are 3 FBGs were used and conducted underwater with a water pump as vibration source that was located underwater. The results show that FBG Accelerometer can be utilized to detect a vibration source located underwater and not limited to air only.

Conclusion

In this paper, FBG Accelerometer characterization has been conducted to detect vibrations underwater as a foundation for developing underwater vibration sensors. The experimental results show that the changes in the peak reflected wavelength (λ_B) of FBG X, Y, and Z decrease with increasing distance. Meanwhile, the experimental results also indicate that as the distance increases, the frequency received by the FBGs decreases as well. Based on linear regressions analysis, $\Delta\lambda_B$ of FBG X decreases linearly with gradient of 0.0058 nm/cm and R-squared value of 92.31%. While $\Delta\lambda_B$ of FBG Y decreases linearly with the gradient of 0.0059 nm/cm and R-squared value of 96.47%. Next, $\Delta\lambda_B$ of FBG Z decreases linearly with the gradient of 0.0045 nm/cm and R-squared value of 98.82%. The results show that FBG Accelerometer can be utilized to detect a vibration source located underwater.

Author Contributions

Conceptualization, Juan Michael Kane Gani; methodology Irwan Kustianto, Retno Wigajatri Purnamaningsih, Sasono Rahardjo; validation, Retno Wigajatri Purnamaningsih; formal analysis, Juan Michael Kane Gani, Retno Wigajatri Purnamaningsih, Sasono Rahardjo; investigation, Juan Michael Kane Gani, Retno Wigajatri Purnamaningsih, Sasono Rahardjo; data curation, Juan Michael Kane Gani; writing—original draft preparation, Juan Michael Kane Gani; writing—review and editing, Juan Michael Kane Gani, Retno Wigajatri Purnamaningsih; supervision, Retno Wigajatri Purnamaningsih, Sasono Rahardjo

Funding

This research received no external funding

Conflicts of Interest

The authors declare no conflict of interest.

References

Dong, L., Xie, W., Wang, C., Zheng, X., Yang, J., Yang, Q., Yin, Y., Wei, W., & Dong, Y. (2023). Enhanced Precision in Frequency and Phase Spectrum in Optical Frequency Domain Reflectometry Using Zoom-FFT Based Spectrum Refinement. *ICAIT 2023 - 2023 IEEE 15th International Conference on Advanced Infocomm Technology*, 312–315. https://doi.org/10.1109/ICAIT59485.2023.10367275

Duggal, R., Gupta, N., Pandya, A., Mahajan, P., Sharma, K., kaundal, T., & Angra, P. (2022). Building structural analysis based Internet of Things network assisted earthquake detection. *Internet of Things*, *19*, 100561. https://doi.org/https://doi.org/10.1016/j.iot.2022.100561

Feng, D., Qiao, X., Yang, H., Rong, Q., Wang, R., Du, Y., Hu, M., & Feng, Z. (2015). A Fiber Bragg Grating Accelerometer Based on a Hybridization of Cantilever Beam. *IEEE Sensors Journal*, *15*(3), 1532–1537. https://doi.org/10.1109/JSEN.2014.2364122

Guo, T., Wang, Y., Li, S., Li, X., & Qiao, X. (2023). High-Sensitivity Three-Axis FBG Accelerometer Based on Elliptical Spring. *IEEE Transactions on Instrumentation and Measurement*, *72*, 1–8. https://doi.org/10.1109/TIM.2022.3228277

Hou, X., Zheng, Y., Jiang, M., & Zhang, S. (2023). SEA-net: Sequence attention network for seismic event detection and phase arrival picking. *Engineering Applications of Artificial Intelligence*, *122*, 106090. https://doi.org/https://doi.org/10.1016/j.engappai.2023.106090

Jena, R., Pradhan, B., Beydoun, G., Alamri, A. M., Ardiansyah, Nizamuddin, & Sofyan, H. (2020). Earthquake hazard and risk assessment using machine learning approaches at Palu, Indonesia. *Science of The Total Environment*, *749*, 141582. https://doi.org/https://doi.org/10.1016/j.scitotenv.2020.141582

Kustianto, I., Purnamaningsih, R. W., Rahardjo, S., Hamidah, M., & Firdaus, M. Y. (2023). Water Temperature Measurement Using Fiber Bragg Grating. *Jurnal Penelitian Pendidikan IPA*, *9*(11), 9341–9345. https://doi.org/10.29303/jppipa.v9i11.3972

Lan, D., Li, J., Chen, J., & Xu, Q. (2022). Floor response spectra of offshore electrical platform under sea waves and earthquake. *Ocean Engineering*, *265*, 112623. https://doi.org/https://doi.org/10.1016/j.oceaneng.2022.112623

Le, H.-D., Chiang, C.-C., Nguyen, C.-N., & Hsu, H.-C. (2023). A 2-D Fiber Bragg Grating Acceleration Sensor Based on Circular Flexure Hinges Structure. *IEEE Transactions on Instrumentation and Measurement*, *72*, 1–11. https://doi.org/10.1109/TIM.2023.3280539

Le, H.-D., Hsu, H.-C., Weng, Y.-Q., Nguyen, C.-N., & Chiang, C.-C. (2022). Design a Fiber Bragg Grating Accelerometer-Based Using a Cantilever Beam Structure. *2022 International Conference on Control, Robotics and Informatics (ICCRI)*, 43–47. https://doi.org/10.1109/ICCRI55461.2022.00014

Li, J., Shen, B., Zhao, D., Zhang, W., & Sun, B. (2022). A High-sensitivity FBG Accelerometer Based on a Bearing. *Journal of Lightwave Technology*, *40*(1), 228–236. https://doi.org/10.1109/JLT.2021.3117867

Li, J., Yang, D., Jiang, Y., Liu, C., Li, X., Zou, J., Chong, Y., Lv, R., Bin, Q., Yan, J., Yuan, P., Ding, X., Li, W., Pan, D., Hao, C., & Li, D. (2023). Cascadable Four-Core Fiber Bragg Gratings Accelerometer for 2-D Low-Frequency Vibration Measurement. *IEEE Sensors Journal*, *23*(19), 22373–22379. https://doi.org/10.1109/JSEN.2023.3298430

Li, Y., Chen, F., Guo, T., Wang, R., & Qiao, X. (2022). Sensitivity Enhancement of Fiber Bragg Grating Accelerometer Based on Short Grating. *IEEE Transactions on Instrumentation and Measurement*, *71*. https://doi.org/10.1109/TIM.2021.3126848

Li, Z. (2021). Recent advances in earthquake monitoring I: Ongoing revolution of seismic instrumentation. *Earthquake Science*, *34*(2), 177–188. https://doi.org/https://doi.org/10.29382/eqs-2021-0011

Made Rai Ratih Cahya Perbani, N. (2018). Deteksi Komponen Frekuensi Rendah pada Tinggi Muka Laut Akibat Pengaruh Gempa Bawah Laut di Stasiun Padang. In *ITB Indonesian Journal of Geospatial* (Vol. 05, Issue 1).

Martínez-Osuna, J. F., Ocampo-Torres, F. J., Gutiérrez-Loza, L., Valenzuela, E., Castro, A., Alcaraz, R., Rodríguez, C., & Ulloa, L. R. (2021). Coastal buoy data acquisition and telemetry system for monitoring oceanographic and meteorological variables in the Gulf of Mexico. *Measurement*, *183*, 109841. https://doi.org/https://doi.org/10.1016/j.measurement.2021.109841

Nguyen, T. T.-V., Le, H.-D., Hsu, H.-C., Nguyen, C.-N., & Chiang, C.-C. (2023). An Optical Fiber Acceleration Sensor Based on a V-Shaped Flexure Hinge Structure. *IEEE Sensors Journal*, *23*(14), 15586–15596. https://doi.org/10.1109/JSEN.2023.3280166

Pan, X., Dong, Y., Zheng, J., Wen, J., Pang, F., Chen, Z., Shang, Y., & Wang, T. (2019). Enhanced FBG Temperature Sensitivity in PbS-Doped Silica Optical Fiber. *Journal of Lightwave Technology*, *37*(18), 4902–4907. https://doi.org/10.1109/JLT.2019.2937138

Parida, O. P., Thomas, J., Nayak, J., & Asokan, S. (2019). Double-L Cantilever-Based Fiber Bragg Grating Accelerometer. *IEEE Sensors Journal*, *19*(23), 11247–11254. https://doi.org/10.1109/JSEN.2019.2936463

Qian, G., Peng, Q., Zhang, Z., Li, M., Wu, K., & Song, Y. (2021). Development of FBG Transformer Vibration Sensor Based on Cantilever Beam Structure. *International Conference on Advanced Electrical Equipment and Reliable Operation, AEERO 2021*. https://doi.org/10.1109/AEERO52475.2021.9708350

Ramdani, F., Setiani, P., & Setiawati, D. A. (2019). Analysis of sequence earthquake of Lombok Island, Indonesia. *Progress in Disaster Science*, *4*, 100046. https://doi.org/https://doi.org/10.1016/j.pdisas.2019.100046

Shen, H., Huang, C., Dong, Y., Wen, J., Zhang, X., Pang, F., & Wang, T. (2023). Radiation Sensitive Long-Period Fiber Grating Based on Tb-Doped Silica Fiber. *IEEE Transactions on Nuclear Science*, *70*(3), 228–234. https://doi.org/10.1109/TNS.2023.3244571

Sianipar, D., Daryono, D., Halauwet, Y., Ulfiana, E., Sipayung, R., Daniarsyad, G., Heryandoko, N., Prasetyo, R. A., Serhalawan, Y., & Karnawati, D. (2022). Intense foreshock swarm preceding the 2019 MW 6.5 Ambon (Seram, Indonesia) earthquake and its implication for the earthquake nucleation process. *Physics of the Earth and Planetary Interiors*, *322*, 106828. https://doi.org/https://doi.org/10.1016/j.pepi.2021.106828

Supendi, P., Sianipar, D., Widiyantoro, S., Rawlinson, N., Daryono, Prayitno, B. S., Gunawan, M. T., Sadly, M., Karnawati, D., Nugraha, A. D., Palgunadi, K. H., Muttaqy, F., & Rahayu, T. (2022).

Analysis of the April 10, 2021 (Mw 6.1) destructive intra-slab earthquake, East Java, Indonesia. *Physics of the Earth and Planetary Interiors*, *326*, 106866. https://doi.org/https://doi.org/10.1016/j.pepi.2022.106866

Teng, Y., Ge, L., Fan, X., Ge, C., & Ma, J. (2024). Dual straight-wing FBG accelerometer for low-frequency vibration measurement. *Optics Communications*, *563*, 130590. https://doi.org/https://doi.org/10.1016/j.optcom.2024.130590

Wang, H., Yan, B., & Liang, L. (2021). A 3D FBG Accelerometer Based on Two Pairs of Flexible Hinges. *IEEE Sensors Journal*, *21*(19), 21586–21593. https://doi.org/10.1109/JSEN.2021.3102035

Wang, L., Xiao, C., Ding, W., Wu, J., & Shi, C. (2022). Application Overview of Fiber Bragg Grating Sensors in Structural Health Monitoring. *IEEE Advanced Information Technology, Electronic and Automation Control Conference (IAEAC)*, *2022-October*, 1946–1950. https://doi.org/10.1109/IAEAC54830.2022.9929863

Wang, X., Guo, Y., Xiong, L., & Wu, H. (2018). High-Frequency Optical Fiber Bragg Grating Accelerometer. *IEEE Sensors Journal*, *18*(12), 4954–4960. https://doi.org/10.1109/JSEN.2018.2833885

Wibowo, A., Purnama, S. R., Pratama, C., Heliani, L. S., Sahara, D. P., & Wibowo, S. T. (2023). Anomaly detection on displacement rates and deformation pattern features using tree-based algorithm in Japan and Indonesia. *Geodesy and Geodynamics*, *14*(2), 150–162. https://doi.org/https://doi.org/10.1016/j.geog.2022.07.003

Xu, Y., Fan, W., Gao, H., & Qiao, X. (2024). Fiber Bragg Grating low-frequency accelerometer based on spring structure. *Optical Fiber Technology*, *82*, 103614. https://doi.org/https://doi.org/10.1016/j.yofte.2023.103614

Yan, B., & Liang, L. (2020). A Novel Fiber Bragg Grating Accelerometer Based on Parallel Double Flexible Hinges. *IEEE Sensors Journal*, *20*(9), 4713–4718. https://doi.org/10.1109/JSEN.2019.2925017

Yang, T., Xiao, Y., Ran, Z., He, X., Shao, T., Wang, W., Li, K., Sun, D., Qin, X., He, Z., Zhang, Y., & Ye, D. (2021). Design of a Weak Fiber Bragg Grating Acoustic Sensing System for Pipeline Leakage Monitoring in a Nuclear Environment. *IEEE Sensors Journal*, *21*(20), 22703–22711. https://doi.org/10.1109/JSEN.2021.3098313

Yang, X., Wei, D., Kou, X., & Huang, J. (2020). Research on Key Technologies of Miniaturization of Fiber Bragg Grating Sensor Signal Demodulation Equipment. *2020 IEEE 5th Information Technology and Mechatronics Engineering Conference (ITOEC)*, 900–903. https://doi.org/10.1109/ITOEC49072.2020.9141679

Zhang, H., Wang, Y., Wen, G., Jia, D., & Liu, T. (2018). Frequency demodulation of dynamic stress based on distributed polarization coupling system. *Journal of Lightwave Technology*, *36*(11), 2094–2099. https://doi.org/10.1109/JLT.2018.2804479

Zhang, L., Liu, M., Hong, L., Li, C., & Zhou, Z. (2022). Design and Optimization of an FBG Accelerometer Based on Single-Notch Circular Flexure Hinge for Medium-Frequency Vibration Measurement. *IEEE Sensors Journal*, *22*(21), 20303–20311. https://doi.org/10.1109/JSEN.2022.3207780